Some Properties of Manganese Oxide (Mn-O) and Lithium Manganese Oxide (Li-Mn-O) Thin Films Prepared via Metal Organic Chemical Vapor Deposition (MOCVD) Technique

Kabir O. Oyedotun[1], Marcus Adebola Eleruja[1], Bolutife Olofinjana[1], Olumide Oluwole Akinwunmi[1], Olusoji O. Ilori[2], Ezekiel Omotoso[1], Emmanuel. Ajenifuja[3], Adetokunbo T. Famojuro[4], Eusebius I. Obianjuwa[3] and Ezekiel Oladele Bolarinwa Ajayi[1*]

1. Department of Physics and Engineering Physics, Obafemi Awolowo University, Ile-Ife 220005, Nigeria

2. Department of Electronic and Electrical Engineering, Obafemi Awolowo University, Ile-Ife 220005, Nigeria

3. Centre for Energy Research and Development, Obafemi Awolowo University, Ile-Ife 220005, Nigeria

4. Department of Chemistry, Obafemi Awolowo University, Ile-Ife 220005, Nigeria

Abstract: Single solid source precursors, Manganese acetylacetonate ($Mn[C_5H_7O_2]_2$) and Lithium manganese acetylacetonate ($Li-Mn[C_5H_7O_2]_3$) were prepared and thin films of Mn-O and Li-Mn-O were deposited on sodalime glass substrates using MOCVD (Metal organic chemical vapour deposition) technique by pyrolysing $Mn[C_5H_7O_2]_2$ and $Li-Mn[C_5H_7O_2]_3$ respectively at a temperature of 420 $^\circ$C for approximately 2 h. The films were characterized using RBS (Rutherford backscattering spectroscopy), SEM (Scanning electron microscopy), XRD (X-ray diffraction), van der Pauw method and Ultraviolet-Visible Spectroscopy. The compositional analysis showed that the Mn:O ratio is 0.2:0.8 while that of Li:Mn:O was found to be 0.47:0.24:0.29. SEM micrograph showed that Mn-O film is composed of hollow needle-like rods with coarse, continuous and uniformly distributed polycrystalline grains rod-like, having average grain size estimated to be below 10μm while those of Li-Mn-O showed that the film is dendritic and polycrystalline in which some of the grains were found to lump together. XRD also showed the polycrystalline nature of the films with orthorhombic MnO_2 and orthorhombic Li_3MnO_4 structures for Mn-O and Li-Mn-O thin films respectively. Results of characterization also showed that the films are semiconducting, highly absorbing in the visible region with absorption edges observed at wavelengths of 525 nm and 550 nm, corresponding to direct optical band gaps of 2.36 eV and 2.25eV for Mn-O and Li-Mn-O thin films respectively.

Key words: MOCVD (Metal organic chemical vapour deposition), metal oxides thin films, precursor, acetylacetonate, bandgap.

1. Introduction

TMO (Transition metal oxides) have continued to receive attention (since the discovery of high temperature superconductors) because of their various interesting properties which make them useful in many scientific and technological applications. For instance, inorganic transparent electrode in the form TMO thin films are used as ECDs (Electrochromic displays) in preference to polymers [1]. However their selectivity as a sensor material is usually poor [2]. Modifying the thin film of the TMO using addition of promoter layer has proved to be a possible way of improving their sensor properties [3]. Discontinuity and hysteresis in conductivity observed in this class of material [4] have also proved to be useful in microcircuitry, computer memory and microelectronics [5].

Manganese can exhibit a number of oxidation states with + 2, + 3 and + 4 being the most common. Other non-stoichiometric oxides have also been observed.

---

*Corresponding author: Ezekiel Oladele Bolariwa Ajayi, Ph.D., professor, research field: material science. Email: eajayi@oauife.edu.ng.

Four crystalline phases with different structures and properties namely MnO, Mn_2O_3, MnO_2 and Mn_3O_4 have been identified for manganese oxide (Mn-O). Except for MnO phase, two or more crystalline modifications can be found in each of the phases. For example, six crystalline modifications designated as α, β, γ, δ, ε and λ can be attributed to the MnO_2 phase in which β-MnO_2 and λ-MnO_2 are stoichiometric variants. Most of the MnO_2 modifications are unstable and need the presence of impurity components like hydroxide, water or alkali constituents in order to be stable [6].

The ability to have different structure and properties together with the ability to accept or donate electrons has led to many applications of manganese oxide. MnO_2 can be used as a catalyst in oxidation of hydrocarbon [7], as electrodes in batteries [8], as energy storage devices in thin film capacitors [9]. Mn_2O_3 can be used in the production of soft magnetic materials [10], as catalyst in various applications [11, 12]. Generally, Mn-O of different stoichiometry can also serve as substrate in the production of some magnetic oxide perovskite materials which possess great magneto-resistance effect and metal-insulator transitions [13, 14]. Such varieties in their structure and in physical and chemical properties make them prime candidate for exploration and study of physical phenomena such as structure-properties relationship in solids.

Portable electronic devices such as laptop, computers, cellular phones, camcorders and so on rely on lithium batteries for power source. Such batteries are also considered as promising candidates for use in electric vehicles. Lithium containing transition metal oxides, Li-M-O (M = transition metal) are attractive as cathode materials in such batteries. Since the commercialization of such batteries, $LiCoO_2$ has been employed as the main cathode materials [15]. The major drawback in the $LiCoO_2$ battery include, high cost and environmental toxicity. As a result, the need to develop new type of cathode materials to replace $LiCoO_2$ cathode will continue to be a major trend in the

development of lithium ion secondary batteries. A potential candidate is the lithium manganese oxide (Li-Mn-O) system since they showed advantage in cost, better acceptable environmental characteristics, high density and working voltage [16, 17].

Extensive work has been performed on the preparation, structure and various properties of the bulk Li-Mn-O system. It has three major compositions, viz, Li_2MnO_4 (cubic), $LiMnO_2$ (orthorhombic or monoclinic) and Li_2MnO_3 (monoclinic) although other non-stoichiometric composition can also exist. Li_2MnO_4 is a spinel material while $LiMnO_2$ is a layered material. In the case of $LiMnO_2$ the monoclinic phase with layered structure is considered very difficult to obtain when compared to the orthorhombic phase which has a zigzag- layered β-phase $NaMnO_2$ structure [17]. Hence, many works were done with the orthorhombic phase.

Improvements in miniaturization of micro and nano electronics and sensor devices such as MEMS (Micro-electro-mechanical systems) technology have reduced the current and power requirements of some of these devices to extremely low level. The fabrication of thin film solid state micro batteries as power sources for these devices is therefore necessary. The major barrier in fabricating a micro battery is to prepare thin film cathode materials using processes compatible with micro electronics fabrication techniques. Such materials in thin film form must have good electrical conductivity and thermal stability without undergoing structural changes.

Various methods of preparing Mn-O and LiMn-O thin film systems have been reported [18-21]. The use of MOCVD (Metal organic chemical vapor deposition) has become one of the most important technique for preparing thin films and coatings of large variety of materials essential to micro electronics fabrication where some of the most sophisticated conditions must be met. Our simple set up has been used in the past to produce good quality thin films that have shown excellent properties. In this study, we report the
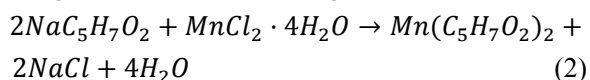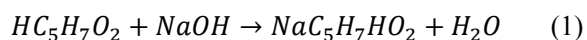
preparation of Mn-O and Li-Mn-O thin films using MOCVD from the pyrolysis of Manganese acetylacetonate ($Mn[C_5H_7O_2]_2$) and Lithium manganese acetylacetonate ($Li\text{-}Mn[C_5H_7O_2]_3$) respectively as single solid source precursors. The use of single solid source acetylacetonates as precursors for the preparation of single and multiple metal oxides has been shown to be convenient by our group [22-24]. The results of the investigations of some of the basic properties of the deposited thin films are also presented.

2. Experiments

2.1 Preparation and Characterization of the Precursors
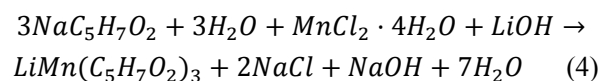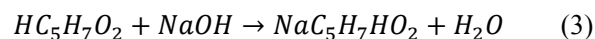
2.1.1 Manganese Acetylacetonate

The precursor for Mn-O thin film manganese acetylacetonate was prepared using the method reported by Ellern and Ragsdale [25]. According to the method, 40 mL of acetylacetone was added slowly to a solution of 16.0 g (0.3 mol) of NaOH in 150.0 mL of water and kept at a temperature below 40 °C to yield sodium acetate. The resulting yellow solution of sodium acetate was added dropwise to a solution of 7.91 g (0.04 mol) of $MnCl_2 \cdot 4H_2O$ in 250 mL of water and stirred vigorously. The resulting yellowish-cream precipitate was filtered off in a Buchner funnel and later dried in an oven at a temperature of 50 °C for about 50 h. The equations of the reactions are given below:

$$HC_5H_7O_2 + NaOH \rightarrow NaC_5H_7HO_2 + H_2O \qquad (1)$$
$$2NaC_5H_7O_2 + MnCl_2 \cdot 4H_2O \rightarrow Mn(C_5H_7O_2)_2 +$$
$$2NaCl + 4H_2O \qquad (2)$$

2.1.2 Lithium Manganese Acetylacetonate

Lithium manganese acetylacetonate was prepared using a modified method of Ellern and Ragsdale [25]. 3.95 g (0.02 mol) of $MnCl_2 \cdot 4H_2O$ was dissolved in water and added to 0.5 g (0.02 mol) anhydrous LiOH (already dissolved in water). The already prepared sodium acetate was then added drop-wise to the solution of $MnCl_2 \cdot 4H_2O$ and anhydrous LiOH over a

period of 2 h. The precipitate was filtered and washed with 7-10 mL of methanol. The precipitate was later dried in an oven at a temperature of 50 °C for 50 h. The reactions are depicted below:

$$HC_5H_7O_2 + NaOH \rightarrow NaC_5H_7HO_2 + H_2O \qquad (3)$$
$$3NaC_5H_7O_2 + 3H_2O + MnCl_2 \cdot 4H_2O + LiOH \rightarrow$$
$$LiMn(C_5H_7O_2)_3 + 2NaCl + NaOH + 7H_2O \qquad (4)$$

2.2 Preparation of Mn-O and Li-Mn-O Thin Films

The thin films of Mn-O and Li-Mn-O were deposited by thermal decomposition of their respective precursors on soda-lime glass substrates using previously reported MOCVD technique by Ajayi et al. [26]. For each deposition, the precursor was ground into fine powder and poured into an unheated receptacle, from where it was blown into the working chamber by nitrogen gas dried over calcium chloride (Fig. 1). The nitrogen gas was bubbled through at a flow rate of 2.5 dm^3 per minute for a period of 2 h. The soda-lime glass substrates were supported on stainless steel blocks for good and uniform thermal contact. In the hot region, the precursor first sublimed in the first chamber and then decomposed at the substrate surface in the second chamber which was electrically heated and maintained at a temperature of about 420 °C. At this temperature, the decomposition of the precursor gave rise to the deposition of the thin films. After the deposition period of 2 h, the gas supply was turned off.

2.3 Characterization of Mn-O and Li-Mn-O Thin Films

RBS (Rutherford backscattering spectroscopy) technique was used to determine the elements present in the films, the stoichiometric ratio of elements in the films and the films thickness. The RBS facility is a 1.7 MeV Pelletron Tandem accelerator of IBM geometry (scattering configuration where the incident beam, surface normal, and detected beam are all coplanar) with integrated beam dose of 10.0 μC. The detector solid angle was 0.833 msr with a resolution of 12 KeV. The incident beam is He+ with energy 2.2 MeV and beam current of 3.8 nA.
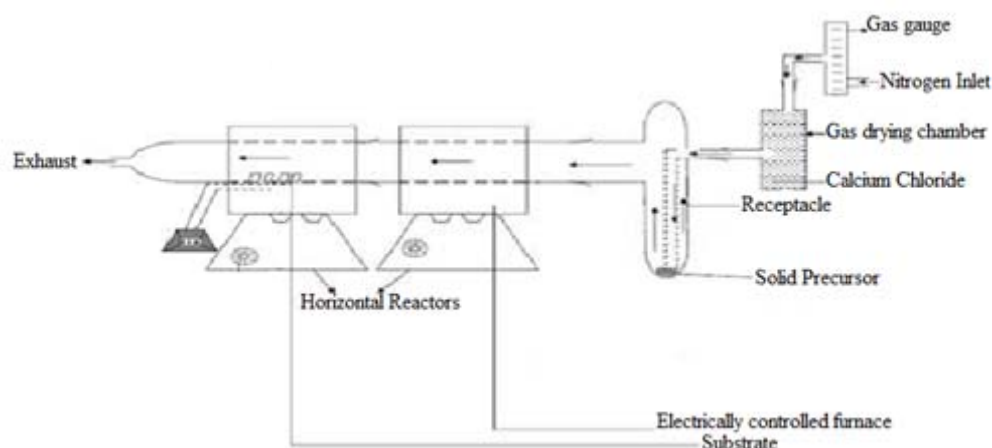
Fig. 1   Schematic diagram of deposition apparatus used for pyrolysis.

The morphology of the films was studied using a Carl Zeiss (model: EVO/MA10) SEM (Scanning electron microscope) equipped with EDX (Energy disperse X-ray) facility for elemental identification. The electron beam of the SEM was 0.1-30 KeV with nominal resolution of 1 nm at 10 KeV.

XRD (X-ray diffraction) of the films were performed with MD-10 model X-ray mini diffractometer using Cu-Kα radiation ($\lambda = 0.15418$ nm). Chemical phase identification was performed using a computer based system with the standard PDF (Powder diffraction file) embedded in the diffractometer. A data base from the International Center for Diffraction Data was also used in comparing the XRD pattern of the films.

The electrical characterization of the film was performed using the four point probe technique with a source current of 1 mA. The four point collinear probe configuration was employed with silver paste at each of the points for ohmic contact. Current-voltage measurement was done using Keithley 2400 Source meter with Rolls and Keener probes. The two outer probes were used to source current while the two inner probes sensed the resulting voltage drop across the sample. The distance of separation between sample probes was 1 cm. A hand lens was used to monitor the probe from puncturing the film.

Absorbance measurements were carried out to study the optical behaviour of the thin films in the range 300-1,100 nm using a PYE-UNICAM SP8 – 400 UV-Visible spectrophotometer. All measurements were made with a blank soda-lime glass substrate in the reference beam. Standardization was done by first replacing the coated substrate with a plain substrate in the sample position; thus we had plain against plain substrate.

3. Results and Discussion

3.1 RBS Analysis of the Films

Compositional analysis of the films was carried out using RBS. RBS was also used to determine the thickness of the films. Fig. 2 shows the RBS spectrum of blank soda-lime glass substrate. The elemental compositions of the soda lime glass substrate were identified as Na, Al, O, Si, S, Cl, K, Ca, Fe and Zn. The RBS spectrum of the Mn-O thin film is shown in Fig. 3. The elements present in the film/glass combination are Mn, O, Na, Al, Si, S, Cl, K, Ca, Fe and Zn. The ratio of Mn and O in the film was found to be Mn:O = 0.2:0.8 while the thickness was estimated to be 1.129×10^{18} atoms/cm^2. In the case of Li-Mn-O thin film, the RBS spectrum of the film/glass combination is shown in Fig. 4, in which the elements present are Li, Mn, O, Na, Al, Si, S, Cl, K, Ca, Fe and Zn. The ratio of Li:Mn:O was estimated to be 0.47:0.24:0.29, while the
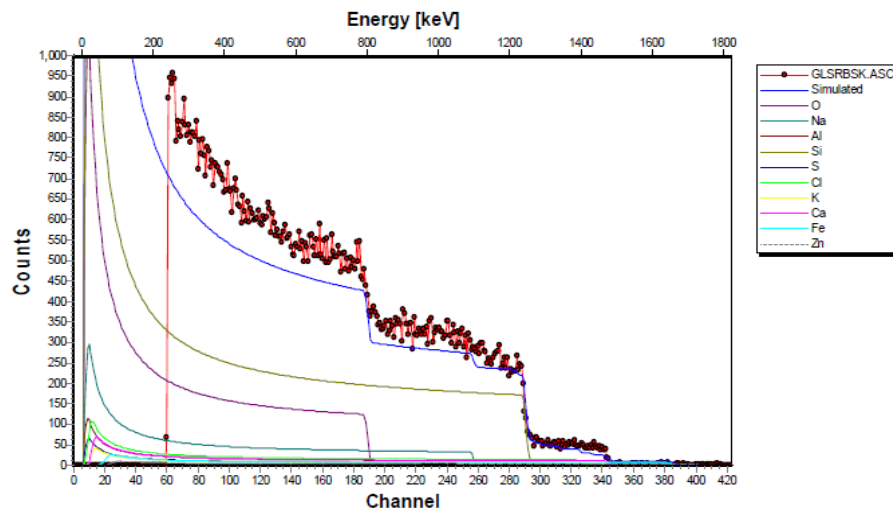
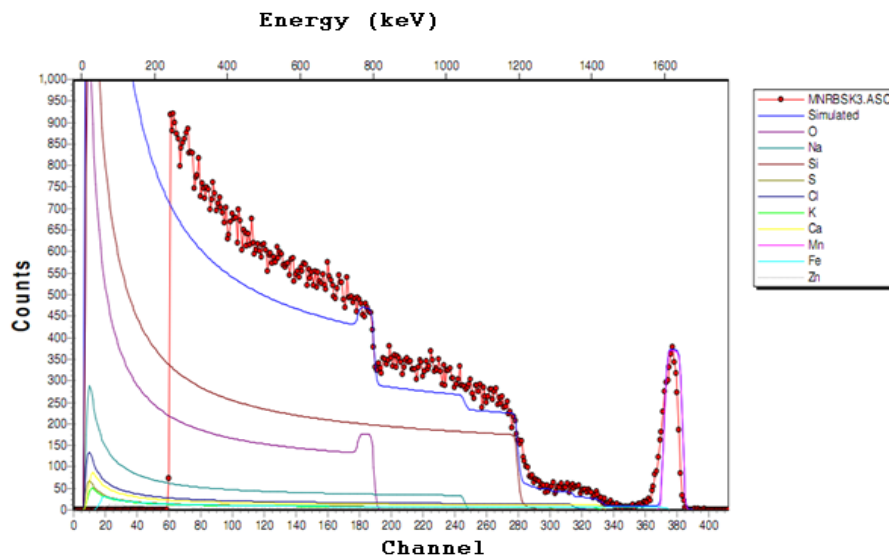**Fig. 2   RBS spectrum of blank soda-lime glass substrate.**

Fig. 3   RBS spectrum of Mn-O thin film/soda-lime glass substrate.
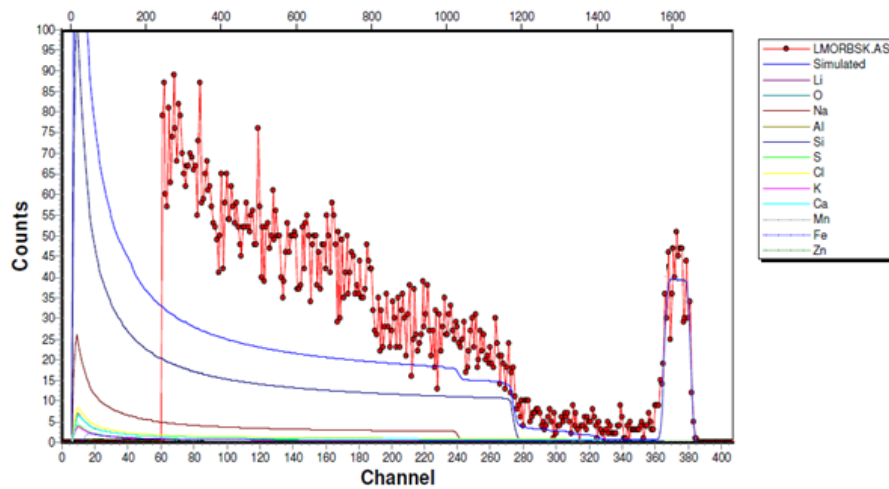

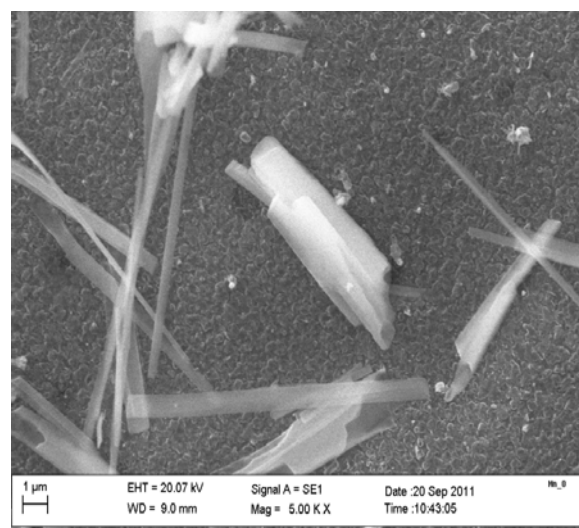**Fig. 4   RBS spectrum of Li-Mn-O thin film/soda-lime glass substrate.**

thickness was estimated to be 6.551×10^{17} atoms/cm^2. This shows that the decomposition of manganese acetylacetonate and lithium manganese acetylacetonate in nitrogen gas medium produced Mn-O and Li-Mn-O thin films respectively in the working chamber. It was also observed that the ratio of Li : Mn in the precursor is different from that of the film. Such difference has been observed in some of our works on mixed metal oxides produced from mechanical mixing of precursors [22-24]. This difference can be attributed to a possible breakdown of the metal-metal bond of the precursor in the vapour phase at the deposition temperature and subsequent reconstitution of the bonds leading to a different stoichiometry of the film.

### 3.2 Surface Morphology and Chemical Characterization of the Films

SEM micrographs of the films obtained from a Zeiss DSM 940 scanning electron microscope are shown in Fig. 5. The SEM is equipped with EDX facility which was used to complement the RBS analysis. The SEM images of the Mn-O thin film (Fig. 5a) showed the morphology to be needle-like rods which are polycrystalline in nature, characteristic of MnO$_2$ [18]. A closer observation of the micrograph showed that the films are composed of hollow needle-like rods with coarse, continuous and uniformly distributed crystalline grains in the background. The grain size was estimated to be less than 10µm. The EDX spectrum is shown in Fig. 6a. The spectrum confirms the presence of the expected elements. Other signals in the spectrum are due to the elements in the soda-lime glass substrate. The EDX analysis also showed non-uniform distribution of Mn and O over the substrate. This may be due to the possible reconstitution of structure and bond during formation stage of the film. Nevertheless, the percentage composition of Mn and O in the deposited film as estimated by EDX is also in agreement with that estimated by RBS.

Fig. 5b showed the micrographs of Li-Mn-O thin films at magnification of 10 KX. The SEM images showed the morphology to be dendritic and polycrystalline. The film has dendrites interspersed within its matrix. Micro cracks which can also be seen may be due to the growth of internal stress during deposition process. Some of the grains were found to lump together as can be seen in the micrograph and may be due to the volume expansion during the formation of the mixed metal oxide thin film. The finger-like dendritic segregation is due to the unusual mobility of lithium in most metal oxides which sometimes result in such dendritic segregation [27]. EDX spectrum (Fig. 6b) of the Li-Mn-O thin film indicates peaks corresponding to Mn and O while other
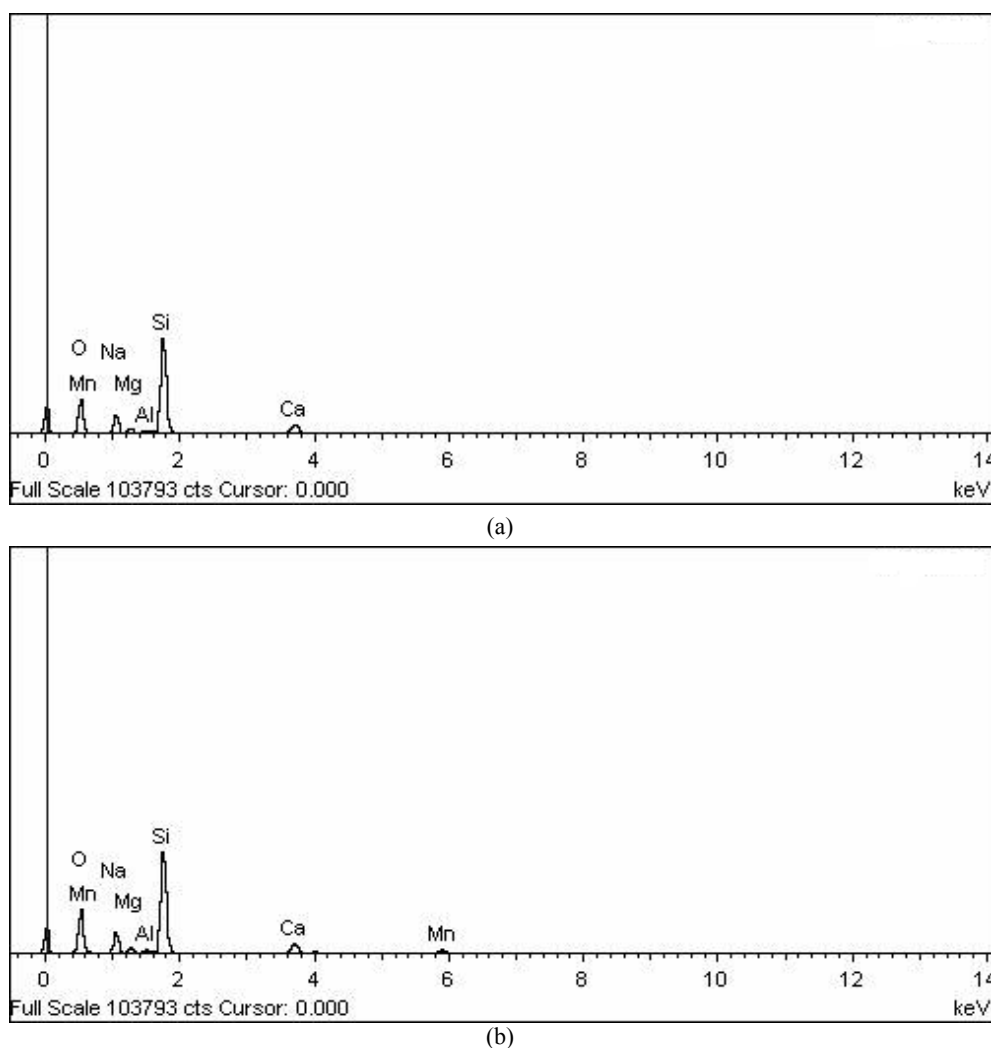

(a)
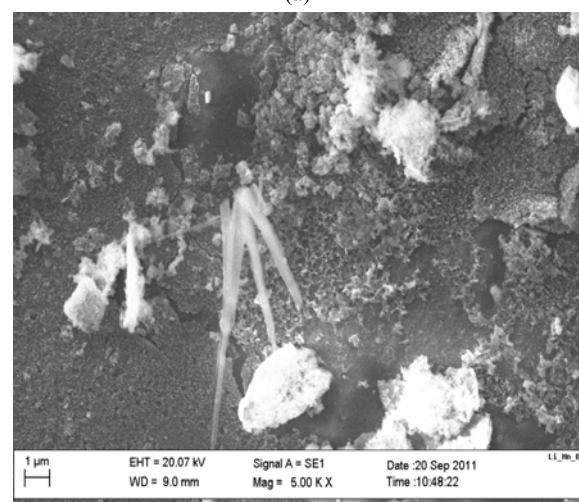
(b)

Fig. 5 SEM Micrograph of (a) Mn-O Thin Film and (b) Li-Mn-O fhin film.

(a)

(b)

Fig. 6 EDX spectrum of (a) Mn-O thin film/soda-lime glass substrate and (b) Li-Mn-O thin film/soda-lime glass substrate.

peaks are due elements in the soda-lime glass substrate. Li could not be detected by this method since EDX cannot detect an element with atomic mass less than that of boron. This ambiguity was however resolved by RBS.

*3.3 X-Ray Diffraction Study of Mn-O and Li-Mn-O Thin Films*

The X-ray diffraction pattern of the films which was collected from MD10 mini diffractometer is shown in Fig. 7. In the case of Mn-O thin film (Fig. 7b), the presence of diffraction peaks in the spectrum indicates that the film is polycrystalline. This was also confirmed by SEM. Diffraction peaks were observed at 2θ values of $19°$, $21.5°$, $27.8°$, $31.4°$, $55.5°$ and $69°$ which

correspond to diffraction planes (200), (101), (201), (301), (212) and (610) respectively (Card Number 43 - 1455). The diffraction pattern clearly indicates orthorhombic MnO_2 structure which is in agreement with what has been reported in the literature [28, 29].

XRD pattern of deposited Li-Mn-O thin film is shown in Fig. 7b. Diffraction peaks, though not well defined, were observed at 2θ values of $23.4°$, $25°$, $27.8°$, $34°$, $41°$ and $43.75°$ which correspond to diffraction lines produced by (101), (021), (121), (131), (141), (122) planes from the orthorhombic Li_3MnO_4 structure (Card Number 32 - 0575). Most authors have reported that their films crystallize into either the orthorhombic $LiMnO_2$ or the spinel $LiMn_2O_4$ structure [30-33], however, to the best of our knowledge crystallization
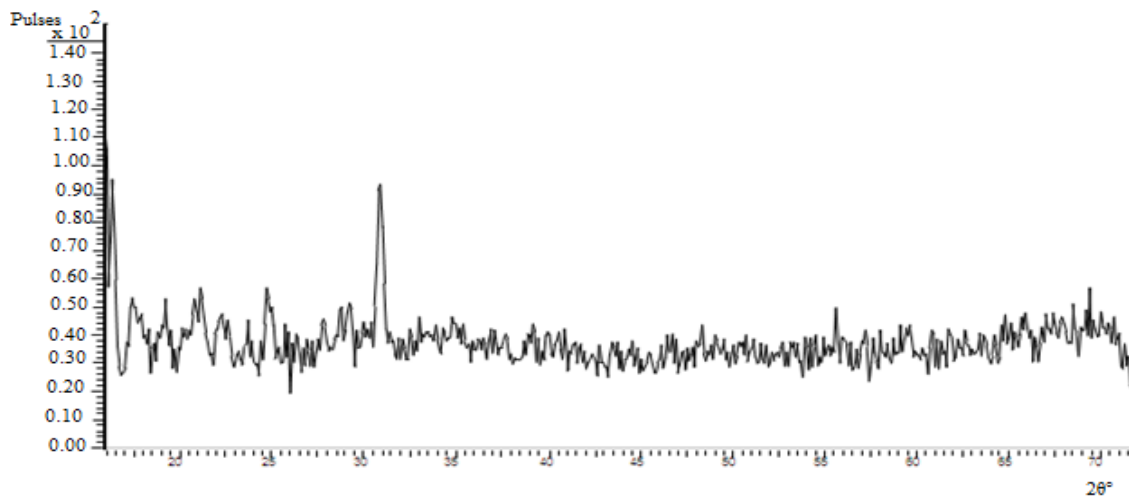
(a)
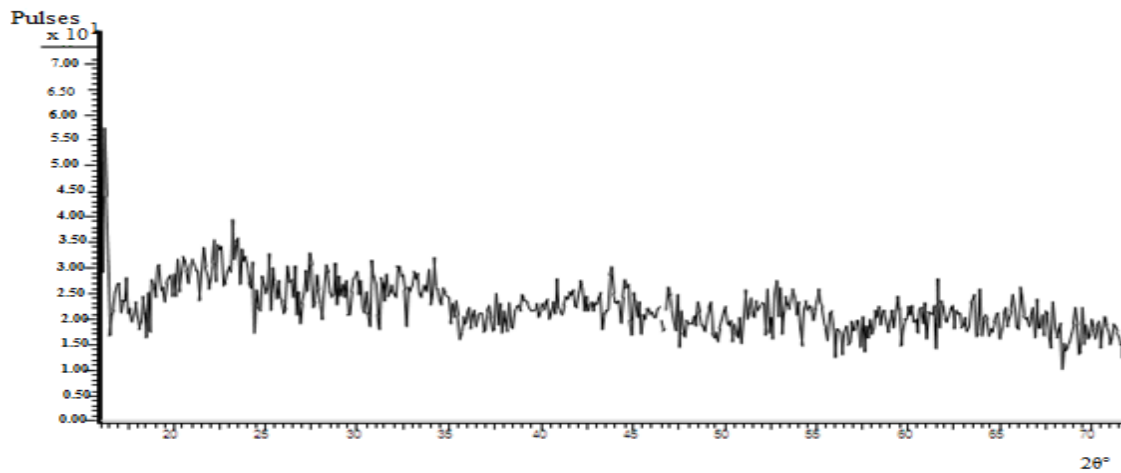
(b)

Fig. 7   X-Ray diffraction pattern of (a) Mn-O thin film and (b) Li-Mn-O thin film.

into orthorhombic Li_3MnO_4 structure is not common. The spectrum also shows that Li-Mn-O thin film has low intense peaks when compared with the spectrum of Mn-O thin film. This may be attributed to the reduction in thickness of the Li-Mn-O film. As a result, the insertion of lithium into the Mn-O matrix has reduced the crystallinity of the Mn-O film as evident from the weak peaks observed in the Li-Mn-O spectrum. Li-Mn-O usually forms an orthorhombic structure as reported [30]. At high temperature, lithium seems to migrate easily and forms precipitate. This unusual mobility in most oxides can also result in a dendritic segregation of lithium in the matrix of the Mn-O system. This was also shown in the SEM micrograph of

Li-Mn-O thin film. A similar feature was reported by Ilori et al. in the case of lithium molybdenum oxide thin film [23].

3.4 Resistivity Measurements of Mn-O and Li-Mn-O Thin Films

The independent measurements of voltage drop and current yielded the film sheet resistivity. The average of the generated currents and voltages by the four-point probes set-up were determined. Sheet resistance R_s, of the films were determined using the equation below:

$$R_s = K\frac{V}{I}\,\Omega/\square \text{ (ohm/square)} \qquad (5)$$

where, K is a constant dependent on the configuration

and spacing of the contacts and is given by:

$$K = \frac{\pi}{ln2} = 4.53 \qquad (6)$$

The resistivity ρ was calculated using the equation,

$$\rho = R_s t \qquad (7)$$

where, t is the film thickness.

For the Mn-O thin film, electrical characterization gave the sheet resistance, (R_s) and resistivity, (ρ) values for Mn-O thin films as 9.144×10^5 ohm/square and 12.4 ohm-cm respectively. The value of the sheet resistance obtained in this work is of the same order of magnitude with those reported in the literature [6, 18]. In the case of Li-Mn-O thin film, the value of 3.63×10^5 ohm/square and 4.9 ohm-cm was obtained for sheet resistance and resistivity respectively. The value of sheet resistance is in agreement with the standard range of 10^5-10^6 ohm/square as earlier reported by Strobel and Charenton [34]. This indicates that both thin films are semiconductors, and are relatively conductive.

The difference in the value of resistivity obtained for Mn-O and Li-Mn-O films is due to the presence of lithium in the latter. In the study of lithium vanadium bronze, such decrease in resistivity was ascribed to a change in structure which is sometimes accompanied by lattice transformation [35]. Analogously, the difference observed here may also be attributed to such change in structure brought about by the insertion of Lithium into the Mn-O matrix. Also, lithium is fully ionized in most Li-metal oxides and donates its electrons to the host bands without changing their structure significantly, which makes it possible to control the band filling of the host material with respect to the lithium content [30]. The mobility of lithium in the Mn-O thin film matrix may also play a significant role in the difference in sheet resistance.

3.5 UV-Visible Spectroscopy Analysis of the Thin Films

The UV-visible spectra for Mn-O and Li-Mn-O thin films respectively deposited at 420 $^{\circ}$C are shown in Fig. 8 respectively. The spectra are plots of absorbance against incident photon wavelength at normal incidence and at room temperature for the thin films.

The UV-Visible spectra show that the films have high absorbance in some parts of the visible region, which decreases gradually as the wavelength increases. The strong absorption can be attributed to either the absorption of some impurities from the substrate, since it is possible for some of the elements of the sodalime glass to diffuse to the surface at the deposition temperature or light scattering from nanometer sized grains of the films [36].The absorption edges lie in the visible region at wavelengths of 525 nm and 550 nm for Mn-O and Li-Mn-O films respectively, which is in agreement with previous reports [29]. The theory of interband absorption and diffusion proposed by Bube [37] states that the fundamental edge and the absorption coefficient should vary according to:

$$\alpha = A\left(\hbar\omega - E_g\right)^n \qquad (8)$$

where, A is a constant of proportionality, E_g the energy of the transition and n a number which characterizes the transition process as either direct allowed ($n = 1/2$) or direct forbidden ($n = 3/2$). Further analysis of the optical data show that a linear region is evident for direct allowed transition ($n = 1/2$) as shown in Fig. 9. The direct band gaps were estimated to be 2.36 eV and 2.25 eV for Mn-O and Li-Mn-O films respectively. The estimated values fall between the values of 1.80-2.45 eV reported for both thin films [29]. Thirumalairajan et al also reported a value of 2.33 eV for manganese oxide obtained from PL and UV-Visible methods [38]. The decrease in band gap is due to the fact that lithium ions must have drifted into the manganese oxide to serve as dopant which appeared to have formed an impurity band within the original band gap of the manganese oxide.

Comparing the band gap of Li-Mn-O thin film with that of Mn-O thin film, there is a narrowing of the forbidding gap due to the inclusion of lithium in the matrix of Mn-O system. The decrease in band gap can be explained using different phenomena. Generally in the family of ternary transition metal oxide (A-M-O),
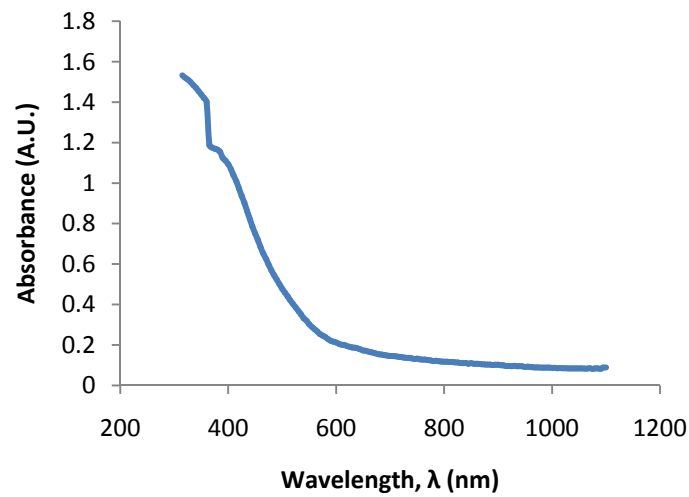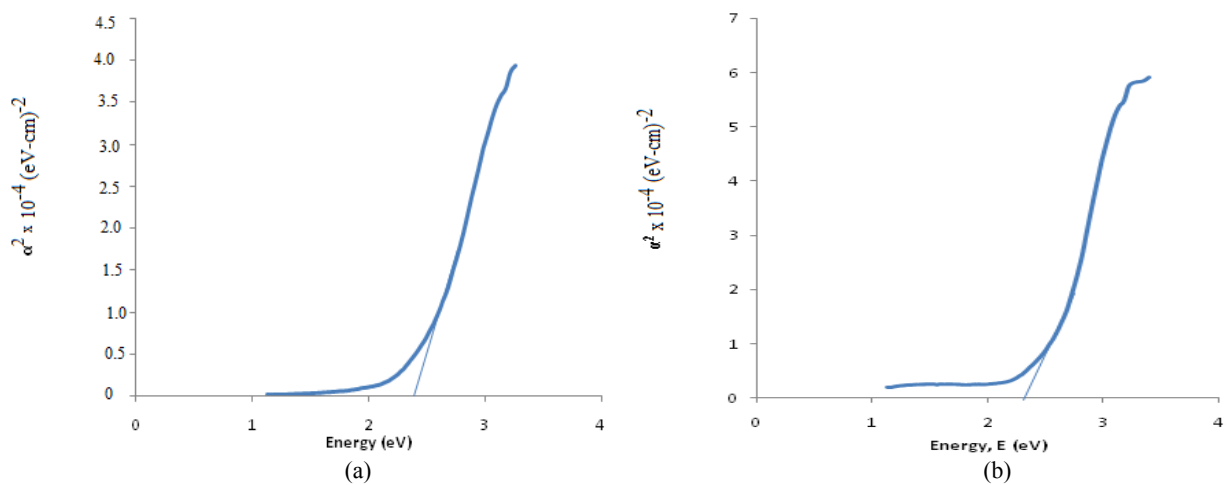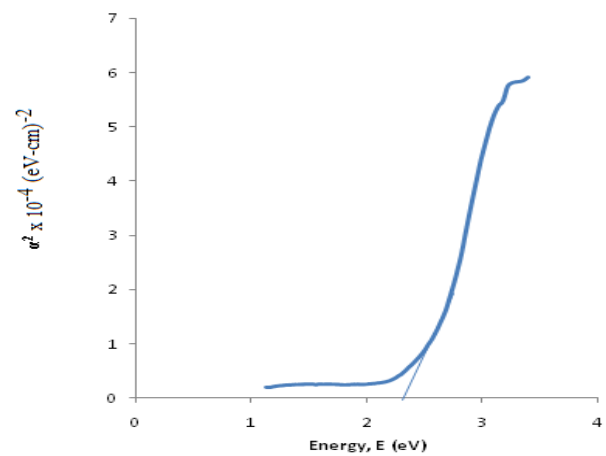
(a)
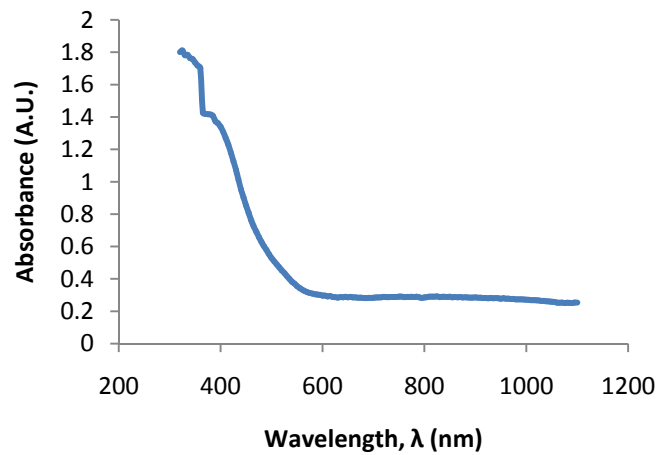
(b)

Fig. 8   Absorbance against wavelength for (a) Mn-O thin film and (b) Li-Mn-O thin film.

(a)

(b)

Fig. 9 α^2 against energy for (a) Mn-O thin film and (b) Li-Mn-O thin film.

alkali metal (A) such as lithium usually donates its outer electrons to the transition metal (M). These electrons can partially fill the π^* conduction band formed by the overlap of t_{2g} 4d-orbitals of the transition metal and p_π-orbit of oxygen making the material to exhibit metallic behavior. However in a situation where the donated electron is localized in the band gap region, an impurity level will be created within the forbidden gap in which electron can then be excited to the conduction band leading to narrowing of the band gap. Good enough also proposed a model for lithium doped transition metals [39]. He proposed that the holes in the oxides occupy φ_e orbit and that the energies of these orbits occupy narrow σ band in the forbidden gap, resulting in the narrowing of the gap. The narrowing of the band gap was also reported in the work on $Li_xMo_yO_z$ thin films [23].

4. Conclusions

In this work, we have prepared single solid source precursors, manganese acetylacetonate ($Mn[C_5H_7O_2]_2$) and lithium manganese acetylacetonate (Li-$Mn[C_5H_7O_2]_3$). Furthermore, we have also shown that it is possible to deposit thin films of manganese oxide (Mn-O) and lithium manganese oxide (Li-Mn-O) on sodalime glass substrate through the pyrolysis of the single solid source precursors by MOCVD technique.

Compositional studies by RBS and EDX confirmed the expected elements in each film. The RBS analysis further gave their stoichiometric ratio of elements in the films. Other characterization also showed that the films are polycrystalline and semiconducting. The films are highly absorbing in most parts of the visible and near infrared regions of the solar spectrum. The films undergo direct transition from valence to conduction band with band gaps of 2.36 eV and 2.25 eV for Mn-O and Li-Mn-O films respectively.

References

[1] Nagai, J. and Morisaki, S. 2003. "Molecular Properties of partially Substituted Nickel Oxide Clusters." *Solid State Ionics* 165 (1-4): 149-53.

[2] Imawam, C., Solzbacher, F., Steffes, H. and Obermeir, E. 2000. "TiO$_x$-Modified NiO Thin Films for H$_2$ Gas Sensors: Effects of TiO$_x$-Overlayer Sputtering Parameters." *Sensors and Actuators* B68 (1-3): 184-8.

[3] Morrison, S. R. 1987. "Selectivity in Semiconductor Gas Sensors." *Sensors and Actuators* 12 (4): 425-40.

[4] Ilori, O. O., Osasona, O., Eleruja, M. A., Egharevba, G. O., Adegboyega, G. A. and Chiodelli, G. et al. 2005. "Preparation and Characterization of Metallorganic Chemical Vapor Deposited Molybdenum (II) Oxide (MoO) Thin Film." *Thin Solid Films* 472 (1-2): 84-9.

[5] Arshak, K. I. and Perrem, R. 1993. "The Correlation of the Electrical and Optical Properties of Thin Films of V$_2$O$_5$-Bi$_2$O$_3$." *J. Phys. D: Appl. Phys.* 26: 1098-102.

[6] Nilsen, O., Fjellvag, H. and Kjekshus, A. 2003. "Growth of Manganese Oxide Thin Films by Atomic Layer Deposition." *Thin Solid Films* 444: 44-51.

[7] Cracium, R. and Dulamita, N. 1997. "Influence of La$_2$O$_3$ Promoter on the Structure of MnO$_x$/SiO$_2$ Catalyst." *Catal. Lett.* 46: 229-34.

[8] Pang, S. C., Anderson, M. A. and Chapman, T. W. 2000. "Novel Electrode Materials for thin Film Ultracapacitors: Comparison of Electrochemical Properties of Sol-Gel Derived and Electrodeposited Manganese Oxide." *J. Electrochem. Soc.* 147: 444-50.

[9] Ammundsen, B., Desilvestro, J., Groutso, T., Hassell, D., Messon, J. B. and Regan, E. et al. 2000. "Formation and Structural Properties of Layered LiMnO$_2$ Cathode Materials." *J. Electrochem. Soc.* 147 (11): 4078-82.

[10] Shao, C., Guan, H., Liu, Y. and Yang, X. 2004. "Preparation of Mn$_2$O$_3$ and Mn$_3$O$_4$ via an Electrospinning Technique." *J. Solid State Chem.* 177 (7): 2628-31.

[11] Ramesh, K., Chen, L., Zhong, Z., Chin, J., Mook, H. and Han, Y. F. 2007. "Preparation and Characterization of Coral-like Nanostructured α-Mn$_2$O$_3$ Catalyst for Catalytic Combustion of Methane." *Catal. Commun.* 8 (9): 1421-6.

[12] Dubal, D. P., Dhawale, D. S., Salunkhe, R. R., Fulari, V. J. and Lokhande, C. D. 2010. "Chemical Synthesis and Characterization of Mn3O4 Thin Films for Supercapacitor Application." *Journal of Alloys and Compounds* 497: 166-70.

[13] Kim, K. J. and Park, Y. R. 2004. "Sol-Gel Growth and Structural and Optical Investigation of Manganese Oxide Thin Films: Structural Transformation by Zn Doping." *J. Cryst. Growth* 270 (1-2): 162-7.

[14] Dagotto, E., Hotta, T. and Moreo, A. 2001. "Colossal Magnetoresistance materials: the Key Role of Phase Separation." *Phys. Rep.* 344 (1-3): 1-153.

[15] Whittingham, M. S., Chen, R., Chirayil, T. and Zavalij, P. 1997. "The Intercalation and Hydrothermal Chemistry of Solid Electrodes." *Solid State Ionics* 94 (1-4): 227-38.

[16] Xia, Y. and Yoshio, M. 1997. "Optimization of Spinel

$Li_{1+x}Mn_{2-y}O_4$ as a 4 V Li-Cell Cathode in Terms of a Li-Mn-O Phase Diagram." *J. Electrochem. Soc.* 144 (12): 4186-294.

[17] Tabuchi, M., Ado, K., Kobayashi, H. and Kageyama, H. 1998. "Synthesis of $LiMnO_2$ with α-$NaMnO_2$ Type Structure by a Mixed Alkaline Hydrothermal Reaction." *Electrochem. Soc. Lett.* 145 (4): L49-52.

[18] Nilsen, O., Foss, S., Fjellvag, H. and Kjekshus, A. 2004. "Effect of Substrate on the Characteristics of Manganese (IV) Oxide Thin Films Prepared by Atomic Layer Deposition." *Thin Solid Films* 468: 65-74.

[19] Isbar, S., Majdalani, E., Tabbal, M., Christidis, T., Zahramam, K. and Nsouli, B. 2009. "Study of Manganese Oxide Thin Films Grown by Pulsed Lase Deposition." *Thin Solid Films* 517:1592-5.

[20] Babu, K. J., Kumar, P. J. and Hussani, O. M. 2013. "Growth, Microstructure and Electrochemical Properties of Rf Sputtered $LiMn_2O_4$ Thin Film on Au/Polyimide flexible Substrate." *Material Science and Application* 4: 128-33.

[21] Jin, S. W. and Wadley, H. N. G. 2008. "Lithium Manganese Oxide Films Fabricated by Electron Beam Directed Vapor Deposition." *J. Vac. Sci. Technol.* A 26 (1): 114-22.

[22] Eleruja, M. A., Egharevba, G. O., Abulude, O. A., Akinwunmi, O. O., Jeynes, C. and Ajayi, E. O. B. 2003. "Preparation and Characterization of Metalorganic Chemical Vapor Deposited Nickel Oxide and Lithium Nickel Oxide Thin Film." *J. Mater. Sci.* 42: 2758-65.

[23] Ilori, O. O., Osasona, O., Eleruja, M. A., Egharevba, G. O., Adegboyega, G. A. and Chiodella, G. et al. 2005. "Preparation and Characterization of Metallorganic Chemical Vapour Deposited $Li_xMo_yO_z$ Using a Single Source Solid Precursor." *Ionics* 11: 387-92.

[24] Mordi, C. U., Eleruja, M. A., Taleatu, B. A., Egharevba, G. O., Adedeji, A. V. and Akinwunmi, O. O. et al. 2009. "Metal Organic Chemical Vapour Deposited Thin Films of Cobalt Oxide Prepared *via* Cobalt Acetylacetonate." *J. Mater. Sci. Technol.* 25 (1): 85-9.

[25] Ellern, J. B. and Ragsdale, C. 1968. "Hexacoordinate Complexes of Bis(2,4-Pentanedeonate) Cobalt(II)." *Inorg. Syn.* 2: 87-92.

[26] Ajayi, O. B. 1970. *Electrical and Optical Properties of Pyrolytically Deposited Indium Oxide Thin Films.* M.Sc. Thesis, University of Illinois, Urbana, Illinois.

[27] Katkova, M. A. and Bochkarev, M. N. 1995. "Dendetric

Polymers Obtained by a Single-Stage Synthesis." *Rus. Chem. Rev.* 64 (11): 1035-48.

[28] Burton, B. B., Fabreguette, F. H. and George, S. M. 2009. "Atomic Layer Deposition of MnO Using Bis(Ethylcyclopentadienyl) Manganese and H_2O." *Thin Solid Films* 517: 5658-65.

[29] Lu, H. L., Scarel, G., Li, X. L. and Fanciulli, M. 2008. "Thin MnO and NiO Films Grown Using Atomic Layer Deposition from Ethylcyclopentadienyl Type of Precursors." *J. Cryst. Growth* 310: 5464-8.

[30] Aydmol, M. K., Koha, A. F., Ceder, G., Cho, K. and Joannopoulos, J. 1997. "*Ab Initio* Study of Lithium Intercalation in Metal Oxides and Metal Dichalcogenides." *Physical Review B* 56: 1354-65.

[31] Zhou, F., Zhao, X., Liu, Y., Li, L. and Yuan, C. 2008. "Size-Controlled Hydrothermal Synthesis and Electrochemical Behaviour of Orthorhombic $LiMnO_2$ Nanorods." *Journal of Physics and Chemistry of Solids* 69: 2061-5.

[32] Moon, H. S., Ji, K. S. and Park, J. W. 2002. "Electrochemical Characteristics of sputtered Lithium Manganese Oxide Thin Film for Micropower Systems." *Journal of the Korean Physical Society* 40 (1):22-5.

[33] Wu, S. H. and Yu, M. T. 2007. "Preparation and Characterization of o-$LiMnO_2$ Cathode Materials." *Journal of Power Sources* 165: 660-5.

[34] Charenton, P. S. 1986. "Electrochemical Lithium Insertion into Layered Manganetes." *Journal of Material Research Bulletin* 28: 93-100.

[35] Gendel, J. 1962. "Magnetic Resonance Studies of Lithium Vanadium Bronze." *Journal of Chemical Physics* 37: 220.

[36] Olofinjana, B., Egharevba, G. O., Eleruja, M. A., Jeynes, C., Adedeji, A. V. and Akinwunmi, O. O. et al. 2010. "Synthesis and Some Properties of Metal Organic Chemical Vapour Deposited Molybdenum Oxysulphide Thin Films." *J. Matr. Sci. Technol.* 26 (6): 552-7.

[37] Bube, R. H. 1974. *Electronic Properties of Crystalline Solids.* Academic Press London, 417.

[38] Thirumalairajan, S., Girija, K., Sudha, M., Maadeswaran, P. and Chandrasekaran, J. 2008. "Structural and Optical Investigation of Manganese Oxide Thin Films by Spray Pyrolysis Technique." *Optoelectronics and Advanced Materials – Rapid Communication* 2: 779-281.

[39] Goodenough, J. B. 1974. "Some Comparison of Fluoride, Oxides and Sulphides Containing Divalent Transition Elements." C.R.N. Rao (Ed.) Marcel Dekker Inc. 215-23.